

A study of the mode I and mode II interlaminar fracture of carbon/epoxy bi-directional composites

P.N.B.Reis^{1,a}, J.A.M. Ferreira^{2,b}, F.V. Antunes^{2,c}, J.D.M. Costa^{2,d}, C. Capela^{3,e}

¹Dep. Engenharia Electromecânica, University of Beira Interior, Covilhã, Portugal

²CEMUC, Dep. Engenharia Mecânica, University of Coimbra, Portugal

³Dep. Engenharia Mecânica, Polytechnic Institute of Leiria, Portugal

^areis@dem.ubi.pt, ^bmartins.ferreira@dem.uc.pt, ^cfernando.ventura@dem.uc.pt,

^djose.domingos@dem.uc.pt, ^eccapela@estg.iplei.pt

Keywords: composites, fracture toughness, finite element analysis, mechanical testing

Abstract. This paper describes an experimental study developed to characterize the mode I and mode II fracture toughness using DCB and ENF tests, respectively. Numerical studies based on finite element method were also developed to obtain to verify the consistence of the experimental results. Significant instantaneous delaminations were observed particularly for the DCB specimen, which were responsible for an oscillatory behaviour of G_{Ic} versus crack length. The maximum load obtained for mode II loading was significantly higher than obtained for mode I loading, with values of 480 and 60 N, respectively. The maximum values obtained for G_{Ic} and G_{IIc} were 500 and 1800 J/m², respectively.

Introduction

Carbon fibre reinforced composite materials are widely used for structural applications of automobile, ships, aircraft, satellite, sportive goods in consequence of its beneficial characteristics, such as stability, lightweight and high stiffness. However, the strength and stiffness of these materials are affected significantly by geometrical and material defects that may result from imperfect manufacturing process or from external loads during the operational life, with consequent limitation to their use in many applications [1-2].

The impact loading can cause extensive delaminations and matrix cracking within the laminates that may not be visible on the surface [3]. For example, impact damage is considered the primary cause of in-service delaminating in composites giving reductions of the compressive residual strength up to 60% [4-5]. Fracture mechanics approaches have been developed to the characterization of delaminating resistance. Particularly, for mode I various standards have been developed for the double cantilever beam (DCB) test covering the measurement of the critical strain energy release rate, G_{Ic} , and several studies can be found [6-8]. Abundant studies are also reported for fracture toughness in mode II, particularly using end-notched flexure (ENF) tests [8-10].

This paper describes an experimental study developed to characterize the mode I and mode II fracture toughness using DCB and ENF tests, respectively. Numerical studies based on finite element method were also developed to improve the consistence of the experimental results.

Material and specimens

The composite plates were manufactured using an epoxy resin and twelve woven balanced bi-directional layers of carbon fibers (196 gr/m²) all of them with the same orientation 0/90°. The resulting plates were 300 mm long, 100 mm wide and 3 mm thick, having a fiber volumetric fraction (V_f) of 0.66. Fibers and resin were hand placed in a mould subjected to a low compression. The mould was put into a vacuum bag during 8 hours for the cure process that occurs at room temperature. The quality control of the plates was done by visual inspections of surface finishing

and void. Figure 1 shows a processed plate with the applied vacuum system. Airtech commercial vacuum consumables were used supplied from SP: peel plies Stitch Ply A in nylon 6-6, release film WL3600 in polypropylene, breather Econoweave 1010W produced with polyester fiber and vacuum bag films WL7400 in PA6. The delamination was simulated with a teflon layer at half of the thickness of the sample. The initial delamination size was 45 mm and the thickness of the teflon layer used was 0.04 mm.

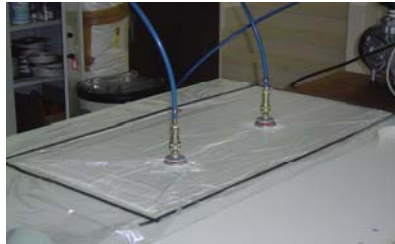


Figure 1. Processed sheet and applied vacuum system.

The experimental work performed involved double cantilever beam (DCB) and end-notched flexure (ENF) tests. The specimens of composite material were cut from the original plates, aligned with one fibre direction: The geometry and dimensions of the specimens are shown in Figure 2. The DCB tests (Fig. 2a) were performed in tension using an electromechanical machine, Shimadzu model AG-X, equipped with a load cell of 1kN, at a strain rate of 1 mm/s. The ENF tests were performed in the same electromechanical machine and with the same strain rate. Figure 2b shows also a schematic view of the three point bending apparatus used and the dimensions of the specimens.

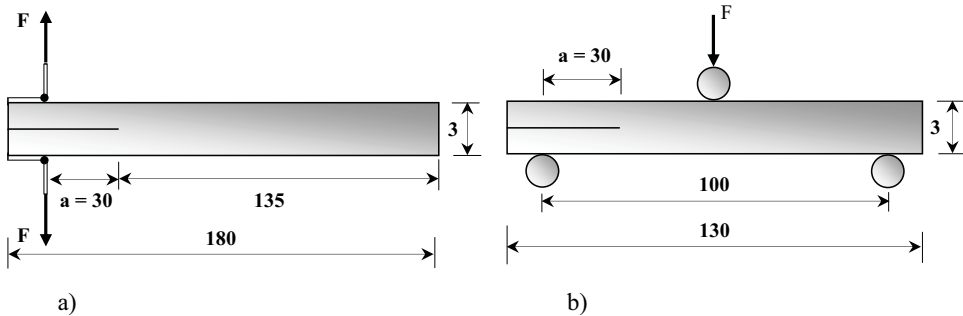


Figure 2. a) DCB specimen (Mode I). b) ENF specimen (mode II). Dimensions in mm.

Determination of elastic properties by the resonant technique

The accuracy of elastic properties is important for the determination of realistic fracture properties. Several experimental techniques have been proposed to determine elastic constants, which can be classified into static and dynamic techniques [11]. The resonant technique, a dynamic technique, is based on the fundamental relation that exists between the elastic properties of a component and its vibratory behavior. Only one specimen is enough to obtain several material constants and average values are obtained, suitable for numerical modeling.

A plate 133.5 mm long, 50 mm wide and 2.03 mm thick was used to obtain the in-plane elastic constants. The specimen was instrumented with a small size extensometer having 120 Ω of electrical resistance and a gauge factor of 2. The extensometer had 2 mm of grid length and a mass of 0.00216 g, so did not affect the resonant frequencies. Careful selection of extensometer position is required to allow the identification of the resonant frequencies associated with different modes. The specimen was suspended on two thin cotton wires to have free-free boundary conditions, and excited by a single elastic strike. The impulse force was not measured, anyway as the mass is low and the specimen remains free-free, relatively low loads were applied avoiding material damage and allowing test repetition on the same specimen. Generally all resonant modes are activated with impulsive loads however it is recommended to impact at anti-nodal positions. The data acquisition system used has a maximum sampling rate of 20x106 samples and a vertical resolution of 12 bits. The operator selects the acquisition time (t_{acq}). Fig. 3 presents a typical response in frequency domain. Table 1 presents the experimental resonant frequencies obtained, where LB, T and TransB stand for Longitudinal Bending, Torsion and Transversal Bending, respectively, as figure 4 illustrates. The longitudinal bending modes are greatly dependent on E_{11} , while the transversal bending modes are greatly influenced by E_{22} , as could be expected. G_{12} influences particularly the torsion modes, while ν_{12} influences the higher order modes (LB3, T3) [12].

Small material portions were weighed in air (P1) and immersed in distilled water at 24 °C (P2), using a Mettler Toledo AG 204 device. Based on the water temperature, its corresponding specific mass value, $\rho=998.5 \text{ kg/m}^3$, is given by the ASTM D792 (ISO 1183). Values of 1414, 1510, 1389, 1405 kg/m^3 ($\rho_{aver}=1430 \text{ kg/m}^3$, $\rho_{ST}=54.4 \text{ kg/m}^3$, $\rho_{ST}/\rho_{aver}=3.8\%$) were obtained with different samples of composite.

Table 1. Experimental resonant frequencies

Mode	Frequency [Hz]	Uncertainty [%]
T1	557.0	0.45
LB1	727.3	0.34
T2	1342.8	0.37
LB2	1953.1	0.26
T3	2588.9	0.19
LB3	3763.8	0.13
TransB1	5238.9	0.19

Table 2. Tension static results(strain rate of 5 mm/s)

E_{11} [GPa]	$(E_{11})_{aver}$ [GPa]	$(E_{11})_{SD} / (E_{11})_{aver}$
57.8		
58.0	58.0	1.2 %
59.0		
57.2		

The finite element method (FEM) was used to replicate the experimental tests, in order to predict resonant frequencies and identify the vibration mode corresponding to each frequency. The materials studied were assumed to be homogeneous, linear elastic and orthotropic. A perfect cuboid geometry was assumed for the specimens, which were supported by low rigidity springs, in order to simulate free-free boundary conditions. Solid isoparametric elements were considered to mesh the geometry. Finally, an iterative procedure was used to calculate the elastic properties from experimental resonant frequencies ($f_{exp, LB1}$, $f_{exp, TransB1}$, $f_{exp, T1}$, $f_{exp, LB3}$). In this approach E_{11} , E_{22} , G_{12} and ν_{12} are successive and independently determined from LB1, TransB1, T1 and LB3, respectively. The properties obtained were $E_{xx}=55.73 \times 10^9 \text{ Pa}$; $E_{yy}=59.067 \times 10^9 \text{ Pa}$; $G_{xy}=4.6 \times 10^9 \text{ Pa}$; $G_{xz}=G_{yz}=1.5 \times 10^9 \text{ Pa}$. The other properties were considered to be: $E_{zz}=5 \times 10^9 \text{ Pa}$; $\nu_{12}=\nu_{13}=\nu_{23}=0.2$.

Static tension tests were also done, to validate the results of the resonant technique. Table 2 presents the results obtained, and an excellent agreement with the resonant technique results is evident.

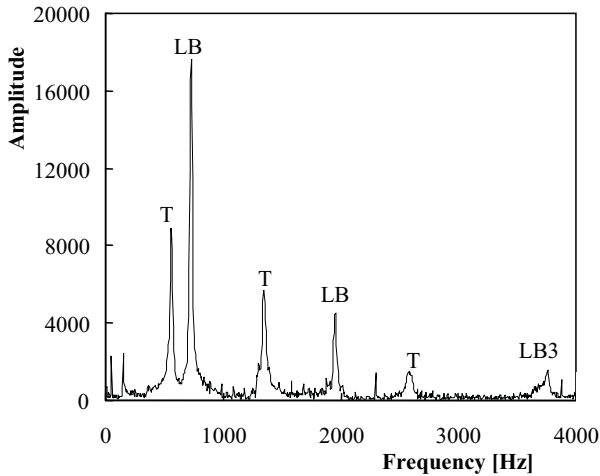


Figure 3. Response in frequency domain.

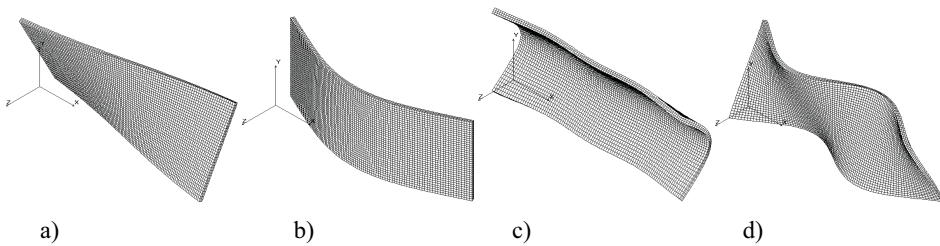


Figure 4. Resonant modes: a) First torsion mode (T1). b) First bending mode (LB1).
c) First transversal bending mode (TransB1). d) Third torsion mode (T3).

DCB specimen

Figure 5 shows the 2D model considered in the determination of mode I energy release rate, G_I , for the DCB specimen. Only half specimen was considered assuming symmetry conditions. The finite element mesh, having relatively small elements near the crack tip, had 1900 nodes and 1800 linear isoparametric elements. Figure 6a) shows the results obtained for plane stress and plane strain conditions. The expression indicated, relating G_I with crack length, fits the numerical results only for relatively large crack lengths. Therefore, the relation established numerically must be used instead.

A sensitivity analysis was developed based on the FEM model in order to understand the influence of different elastic properties on G_I . The non dimensional sensitivity was defined as:

$$\Delta G = \frac{\partial G}{\partial E_{ij}} \cdot \frac{E_{ij}}{G} \quad (1)$$

Notice that a sensitivity of 0.5 indicates that a variation of 1% in E_{ij} produces a variation of 0.5% in G [13]. The results, presented in Fig. 6b), indicate a great influence E_{11} , with a non-dimensional

sensitivity of about 1. G_{12} for relatively short cracks and ν_{31} have a sensitivity one order of magnitude lower. The other elastic properties have a negligible influence on G_I .

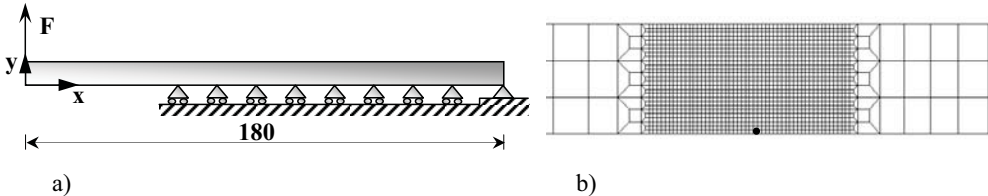


Figure 5. a) Physical model of DCB specimen (W=1 m). b) Detail of near crack tip mesh.

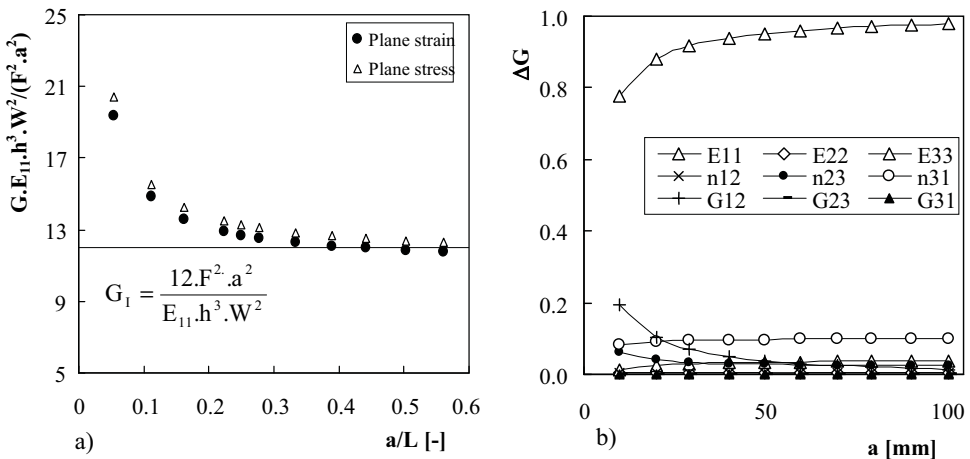


Figure 6. DCB specimen. a) G_I versus crack length. b) Non-dimensional sensitivity (plane strain).

A 3D finite element analysis was also developed to obtain the variation of G_I along crack front. Figure 7b shows the distribution of energy release rate for a straight crack. A great variation is obvious, with lower values near the surface, which indicates that the straight crack is not the natural shape [14]. The crack adapts its shape in order to have a constant driving force along whole front. A curved delamination front develops, with the surface region delayed relatively to the center of the specimen. A curved cracked front was considered, as figure 7a illustrates, with a delay at surface of 1.4 mm. The results of figure 7b show that this small variation of crack shape is enough to obtain a nearly constant distribution of G_I along crack front. In fact, an order of magnitude exists between crack shape variations and G_I variations [15].

ENF specimen

Figure 8a shows the 2D model considered in the determination of mode II energy release rate, G_{II} , for the ENF specimen. A friction coefficient of 0.35 was considered between the crack faces, which is according the results obtained by Davidson and Son for carbon-epoxy composites [16]. Anyway, the influence of the friction was observed to be negligible in ENF tests [16,17]. Figure 8b shows the variation of mode II energy release rate (G_{II}) with crack length. The results are relatively close to the

analytical expression presented, however a significant difference is observed when the crack extends ahead of specimen's center, where the load is applied.

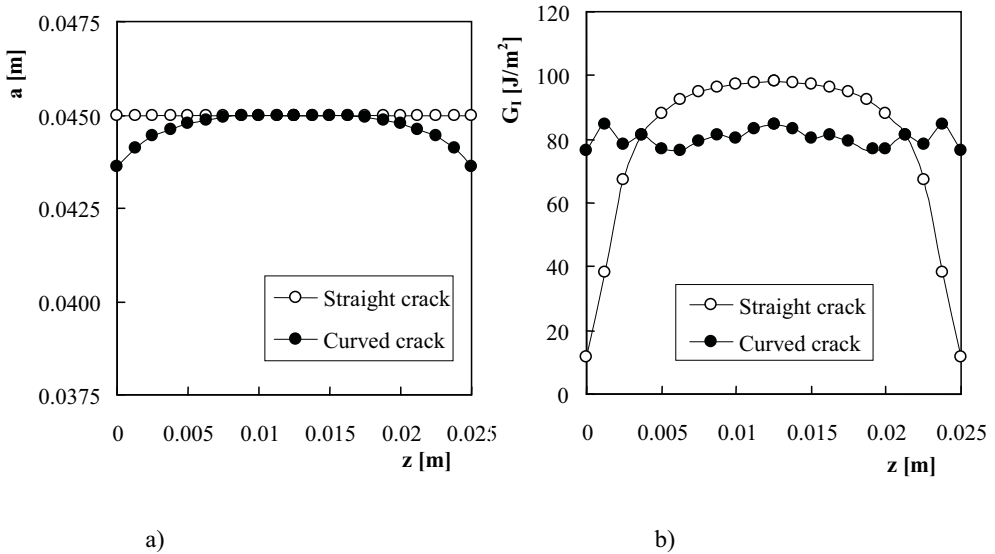


Figure 7. a) Crack shapes. b) G_I along crack front ($a_{max}=45$ mm; $W=25$ mm, $F=10$ N).

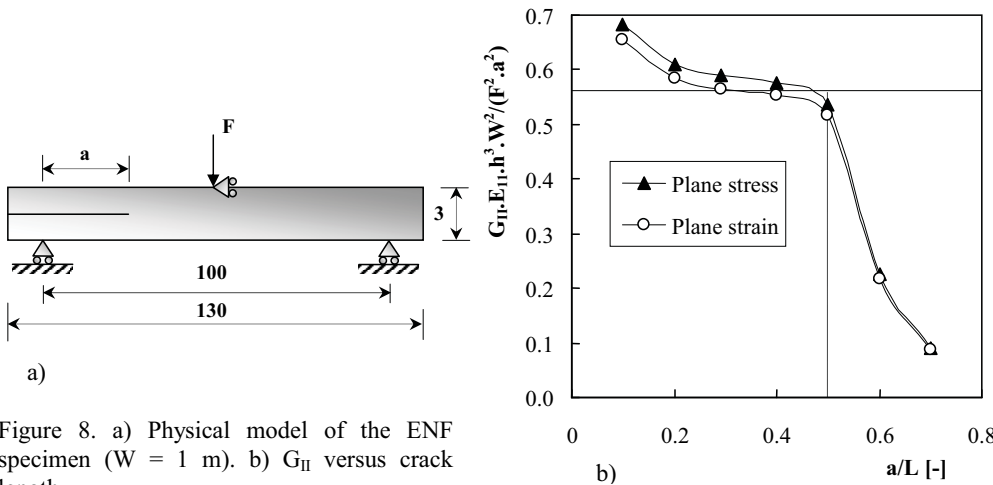
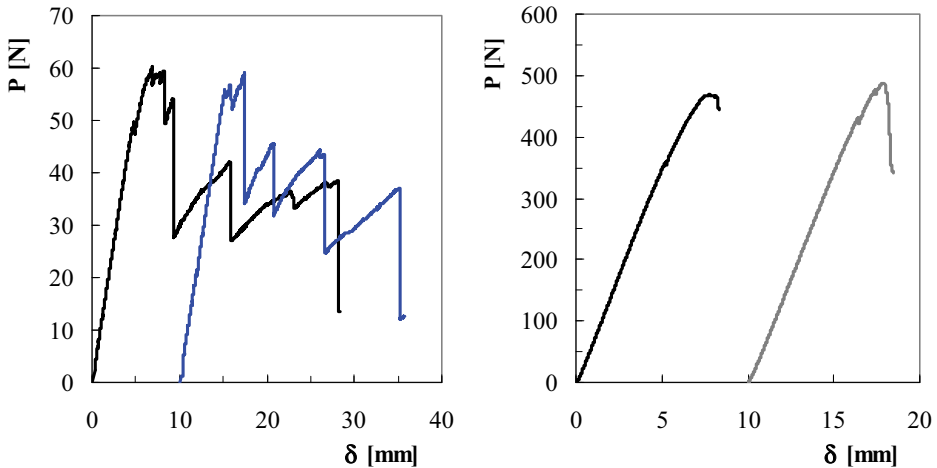


Figure 8. a) Physical model of the ENF specimen ($W = 1$ m). b) G_{II} versus crack length.

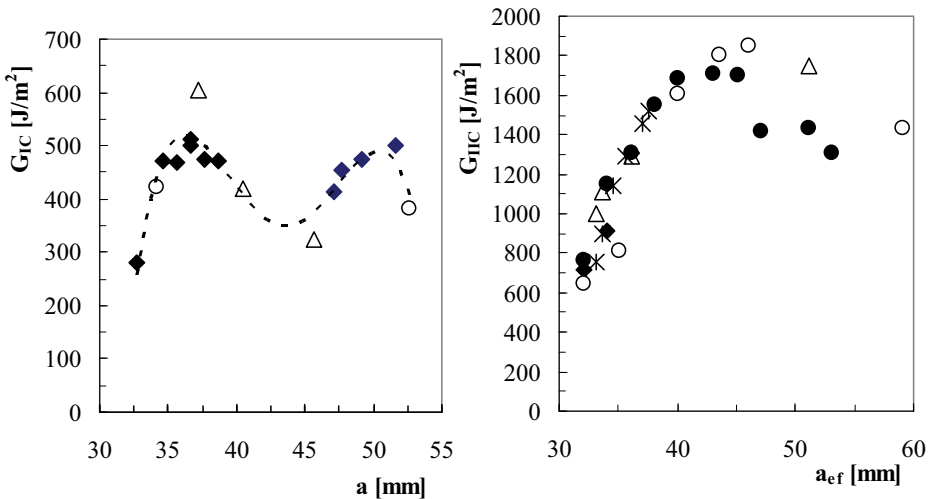
Experimental results

Figure 9 presents typical experimental load-displacements curves obtained in the DCB and ENF tests. These curves were found to be are reproducible and similar to literature results. In mode I particularly, load drops are evident indicating large instantaneous delaminations. As a consequence, the crack length measurement was found to be difficult, therefore a large scatter was observed. For mode II specimens, instantaneous delaminations were also observed but less significant. Figure 10

presents the energy release rate for mode I and mode II specimens. The formulation used to obtain G can be found in the work of Morais and Pereira [18]. For the DCB specimen the peak of G_{Ic} was obtained at a crack length of 35 mm. The curve has an oscillation behaviour, which is explained by the significant instantaneous delaminations evident in figure 9a). The G_{Ic} results obtained with the ENF specimen show a stable increase up to the peak value observed for an effective crack length of about 43 mm. The maximum values obtained for G_{Ic} and G_{IIc} were 500 and 1800 J/m^2 , respectively.



a) b)
Figure 9. Typical load-displacement curves for: a) DCB tests, b) ENF tests.



a) b)
Figure 10. a) G_{Ic} versus crack length; b) G_{IIc} versus crack length.

Conclusions

The delamination of carbon-epoxy laminated composites was studied using mode I DCB specimen and mode II ENF specimen. Notched specimens were prepared and tested under quasi-static loading. The elastic constants of the composite were determined using the resonant technique. A 2D numerical model was developed to obtain the relations between G_I and crack length, and empirical relations were defined for plane stress and plane strain conditions. A 3D finite element model was developed and it was found that the straight crack is not the natural shape. The iso-G crack shapes are curved cracks with a relatively small tunneling parameter. Experimental testing was developed to obtain the load-displacement curves and energy release rate versus crack length. Significant instantaneous delaminations were observed particularly for the DCB specimen. The maximum load obtained for mode II loading was significantly higher than obtained for mode I loading, with values of 480 and 60 N, respectively. The mode I critical energy release rate showed an oscillatory behaviour, explained by the instantaneous delaminations. The maximum values obtained for G_{Ic} and G_{IIc} were 500 and 1800 J/m², respectively.

Acknowledgement

The authors would thank by NATO Research & Technology Organization for sponsoring the work reported.

References

- [1] F. Collombet, J. Bonini and J.L. Lataillade: *Int. J. Numer. Meth. Engng.* Vol. 39 (1996), p. 1491.
- [2] W.O.W. Richardson and M.J. Wisheart: *Compos. Part A-Appl. S.* Vol. 27 (1996), p. 1123.
- [3] R.D. Adams and P.D. Cawley: *NDT&E Int.* Vol. 21 (1998), p. 208.
- [4] M.F.S.F. de Moura and A.T. Marques: *Compos. Part A-Appl. S.* Vol. 33 (2002), p. 361.
- [5] S. Zheng and C. Sun: *Eng. Fract. Mech.* Vol. 59 (1998), p. 225.
- [6] T.E. Tay: *Appl. Mech. Rev.* Vol. 56 (2003), p. 1.
- [7] A.B. Pereira, A.B. de Morais, M.F.S.F. de Moura and A.G. Magalhães: *Compos. Part A-Appl. S.* Vol. 36 (2005), p. 1119.
- [8] A.B. Pereira and A.B. de Morais: *Compos. Part A-Appl. S.* Vol. 39 (2008), p. 322.
- [9] M.A.L. Silva, M.F.S.F. de Moura and J.J.L. Morais: *Compos. Part A-Appl. S.* Vol. 37 (2006), p. 1334.
- [10] P. Davies, G.D. Sims, B.R.K. Blackman, A.J. Brunner, K. Kageyama, M. Hojo, K. Tanaka, G. Murri, C. Rousseau, B. Gieseke and R.H. Martin: *Plast. Rubber Compos.* Vol. 28 (1999), p. 432.
- [11] M. Radovic, E. Lara-Curzio, and L. Riester: *Materials Science and Engineering A* Vol. 368 (1-2) (2004), p. 56.
- [12] F. Antunes, A. Ramalho, J.A.M. Ferreira, C. Capela and P.N.B. Reis: *Journal of Testing and Evaluation* Vol.36(1) (2008), p.89.
- [13] D. Tortorelli and P. Michaleris: *Inverse problems in Engineering* Vol. 1 (1994), p. 71.
- [14] A.B. Morais, C.C. Rebelo, P.M.S.T. de Castro, A.T. Marques and P. Davies: *Fatigue Fract Engng Mater Struct* Vol. 27 (2004), p.767.
- [15] R. Branco and F.V. Antunes: *Eng. Fract Mech* (2008), doi:10.1016/j.engfracmech.2007.12.012
- [16] B.D. Davidson and X. Sun: *J Reinf Plastics Compos* Vol. 24 (2005), p. 1611.
- [17] A.B. Morais and M.F.S.F. Moura: *Eng. Fract Mech* Vol. 73 (2006), p. 2264.
- [18] A.B. Morais and A.B. Pereira: *Compos. Part A-Appl. S.* Vol. 38 (2007), p. 785